Numerical and experimental investigation of a piston thermal barrier coating for an automotive diesel engine application

Paper Proposal

Possible Journal: Applied Thermal Engineering
https://www.journals.elsevier.com/applied-thermal-engineering

AUTHORS:
Sabino Caputo, Federico Millo, Giulio Boccardo, Andrea Piano (Politecnico di Torino)
Giancarlo Cifali, Francesco Concetto Pesce (GM-GPS)

TITLE: "Numerical and experimental investigations of a piston thermal barrier coating for an automotive diesel engine application"

ABSTRACT:

Numerous research activities in diesel engine field are directed towards improvement of the engine efficiency through the thermally insulated combustion chamber. This paper investigates the potential of coated pistons in reducing fuel consumption and pollutant emissions of a 1.6 l automotive diesel engine. After a literary review on the state-of-the-art of the materials used as Thermal Barrier Coatings (TBCs) in engine field, anodized aluminum has been selected as the most promising one. In particular, it presents very low thermal conductivity and heat capacity which ensure a high wall temperature swing property. Successively, numerical analysis by utilizing a one-dimensional Computational Fluid Dynamics (CFD) engine simulation code was carried out to investigate the potential of the anodized aluminum as piston TBC. The simulations have highlighted the potential of up to about 1% in Indicated Specific Fuel Consumption (ISFC) and 6% in heat transfer reduction. To confirm the simulation results, the coated piston technology has been experimentally evaluated on a prototype engine and compared with the baseline aluminum pistons. Despite the promising potential for ISFC reduction highlighted by the numerical simulation, the experimental campaign has indicated a slight worsening of the engine efficiency (up to 2% at lower load and speed) due to the slowdown of the combustion process. The primary cause of these inefficiencies is attributed to the roughness of the coating.

KEYWORDS: Low Heat Rejection Engine, engine insulation, thermal barrier coating, piston coating, diesel engine, engine efficiency.

1 Introduction

In the current automotive industry scenario, where the CO_2 targets, set by the new regulations, are becoming more and more demanding, the use of advanced technologies, as thermal insulation, is getting realizable. The idea of the so-called Low Heat Rejection Engines (LHREs), namely engines with reduced in-cylinder heat losses, is not new, but it was introduced in the 80's to improve the internal combustion engine efficiency. In the past, LHREs were realized by covering the combustion chamber surfaces (i.e., pistons, valves, ports) with ceramic materials, such as zirconia and silicon nitride, which present lower thermal conductivity than the conventional metals, and thereby can operate at higher temperatures, insulating the engine. Nevertheless, many research works were focused on this concept [1–8], the final results were often inconclusive and contradictory, not facilitating the market penetration of the technology. A crucial limitation for the traditional ceramic coating was the reduction of the engine volumetric efficiency, caused by the higher wall temperature during the entire engine cycle (including the intake phase), and the relative performance deterioration [6,9]. Furthermore, increments in pollutant emissions (especially NO_x), due to the higher wall temperatures, were assessed in many research works [5,10–12]. Many other authors found out that, due to the higher wall temperatures, a shorter ignition delay occurs in LHREs, causing a decrease in the premixed combustion and a corresponding increase in the amount of fuel burned during the late combustion phase [13–17]. Thus, since the heat release shifted to late phase in the cycle, less useful work would be obtained from the LHRE. In particular, many researchers [13,17–19] have discovered that using a suitable retarded injection timing it is feasible to partially compensate the detrimental effect of insulation on heat release rate and NO_x emissions.

Another way to overcome these issues was recently proposed by Toyota [20–23], introducing the wall "temperature swing" concept and developing an anodizing aluminum with silica filler as Thermal Barrier Coating (TBC). Thanks to the low thermal conductivity and heat capacity of the coating, the wall temperature is able to follow the oscillations of the in-cylinder gas temperature, causing heat insulation during the combustion and preventing the intake air heating. The main problems derived from anodized aluminum coatings, and in general from other ceramic coatings, are their higher surface roughness and porosity, which can slow down the combustion and compromise the engine efficiency gains [15,20,24,25].

The objective of the present study was to investigate the effects of the TBC technology applied on diesel engine pistons. In the first part of this article, the thermos-physical characteristics of the traditional and the innovative TBCs are reviewed and compared. Then, using a one-dimensional CFD numerical model, the anodized aluminum material was selected as the most promising TBC for reducing heat transfer and improving engine efficiency. In the last part of this research, the selected coating was tested on a 1.6 liters, automotive diesel engine.

2 State-of-the-art of Thermal Barrier Coatings for engine applications

A Thermal Barrier Coating (TBC) is a particular superficial coating able to protect the metallic substrate against the thermal loads produced in high-temperature applications, i.e., internal combustion engine and turbomachines.

Usually a TBC structure presents a thick ceramic layer called Top Coat (TC), which has a very low thermal conductivity and so acts as a thermal insulator element, and an intermediate metal alloy layer, called Bond Coat (BC), which is thinner than the TC and it is used to reduce the difference of the linear Thermal Expansion Coefficient (CTE) between the metal substrate and the ceramic part of the coating.

The bond coat is usually made by a metallic Cobalt-based (CoNiCrAlY) or Nickel-based (NiCoCrAlY) superalloy, which contain Chromium and Aluminum elements, useful for the Thermally Grown Oxide (TGO) formation at the TC/BC interface, and Yttrium to facilitate the adhesion of the TGO layer to the bond coat.

The top coat is often constituted by a ceramic material that is able to fulfill with the following properties:

1. high melting point;
2. chemical stability (avoid reactions);
3. phase stability (avoid phase transformations);
4. low thermal conductivity;
5. low heat capacity;
6. good thermomechanical properties;
7. good adherence to the BC;
8. low sintering rate;
9. toughness;
10. hardness and good resistant to erosion wear.

2.1 Traditional Thermal Barrier Coatings

In the automotive research, zirconia (ZrO_2) has been the widest employed TC material, in particular with an yttria content of about 7-8 wt.%, obtaining the so-called Yttria Stabilized Zirconia (YSZ). Other materials, as the refractory mullite and the pyrochlore, were taken into consideration by recent researches [26,27] as a valid alternative to YSZ.

The characteristics of Yttria Stabilized Zirconia (YSZ) are: high fracture toughness, low thermal conductivity, and relatively high CTE, closer to that of the metallic substrate. Besides, YSZ cannot be used in the high temperature applications, because of the destabilization of the material and the consequent internal stress formation.

Mullite is an intermediate stable compound of alumina and silica with stoichiometry $3Al_2O_3 \cdot 2SiO_2$. In comparison with YSZ, mullite has a lower CTE and a higher thermal conductivity. The very low CTE leads to a higher thermal

expansion mismatch with the metal substrate, but also allows to strongly reduce the stresses due to the thermal gradient generated throughout the layer. In a diesel engine, the latter feature is decisive because the coating thicknesses are greater and the stresses generated can cause failures. However, the main reason that makes mullite a very suitable alternative to YSZ is its superior resistance to creep, that is the main cause of superficial traction tensions and damages of zirconia [28,29]. The greater creep resistance gives to the mullite coatings a better thermal shock resistance and a more prolonged thermal fatigue life than the YSZ in the operating conditions of diesel engine components. The thermal properties of YSZ and mullite are reported in Table 1.

	T [°C]	Thermal conductivity [$Wm^{-1}K^{-1}$]	Specific heat [J/mol K]	CTE [$x10^{-6}$ K^{-1}]
YSZ	27	0.67	420	7.5
	727	0.58	547	9
	1227	0.56	569	9.7
Mullite	27	1.32	838	5.1
	727	1.32	1202	5.2
	1227	1.34	1219	5.5

Table 1. Thermal properties of YSZ and mullite at three different temperatures [30].

2.2 Innovative Thermal Barrier Coatings & "Temperature Swing"

Beyond the traditional ceramic thermal barrier coatings, new researches are focused on new innovative materials able to exploit the so-called wall "temperature swing" property.

In more detail, the convective heat flux Q from the in-cylinder gas through the combustion chamber walls is calculated by Eq. 1:

$$Q = A \cdot h_g \cdot (T_{gas} - T_{wall}) \quad (1)$$

where, A is the combustion chamber surface, h_g is the convective heat transfer coefficient, T_{gas} is the in-cylinder gas temperature and T_{wall} is the wall temperature.

The so called "Temperature Swing" concept is a heat loss reduction technology that reduces the temperature difference between in-cylinder gas and surrounding walls, by quickly changing the wall temperature, following the transient gas temperature. A sketch of gas and surface temperatures during the entire engine cycle, for different combustion chamber wall materials is reported in Figure 1. Three surface temperatures are plotted, corresponding to: a conventional wall (metal), a conventional ceramic insulation wall (i.e., YSZ) and a "temperature swing" insulation wall.

The surface temperatures for the metals commonly used for combustion chamber (aluminum or iron alloy), which are characterized by high thermal conductivity, remain almost constant during the entire engine cycle. Conventional ceramic insulations present higher temperatures during the entire engine cycle, including the intake stroke. This fact results in reducing heat transfer during the combustion, but also in a decrease in the volumetric efficiency, deterioration in power, increase in the working gas temperature and exhaust emissions.

In the case of "temperature swing" insulation, the surface temperature of the coating, which is characterized not only by low thermal conductivity but also by low heat capacity, is able to fluctuate following the in-cylinder gas temperature. With this technology, not just the heat losses during the combustion and expansion strokes can be reduced, thanks to the higher coating surface temperature, but also the intake air heating and the volumetric efficiency decreasing are avoided, due to the cooled coating temperature during the intake and compression phases.

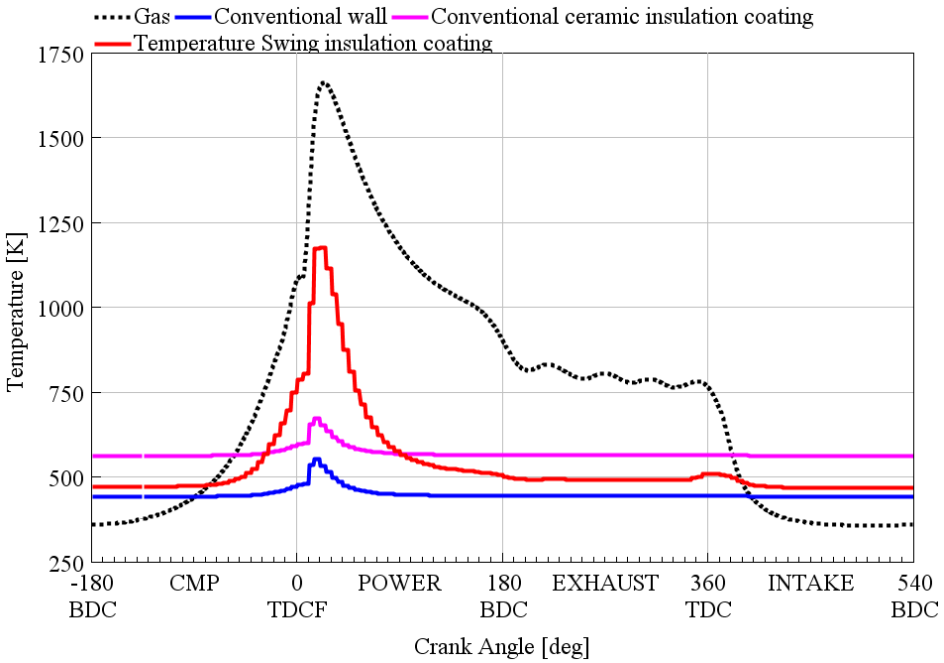

Figure 1. Gas and wall temperature profiles during the engine cycle

Toyota [20–23] recently developed and proposed a new material, called Silica Reinforced Porous anodized Aluminium (SiRPA), as piston TBC. The coating is realized with the anodization of an aluminium alloy (Al-12% silicon), and is characterized by a layer of aluminium oxide with a structure containing cylindrical channels with diameters of nanometer size (10-30 nm) oriented perpendicular to the surface and constituting the structure nanometer porosity. In the structure, silicon crystals are also present, that disturb the nano-channel growth and constitute the micrometer porosity (1-10 μm). Moreover, through a post-treatment, a surface silica layer of a few microns is applied as a sealant, to prevent the penetration of the hot in-cylinder gasses inside the channels [21, 22].

The high porous structure makes the coating density very low, which is a key factor for thermal swing concept. As shown in Eq. 2 and 3, both the thermal

conductivity (λ) and the volumetric specific heat capacity (c_v) directly depend on the material density (ρ).

$$\lambda = \rho \cdot C \cdot \kappa \quad (2)$$

$$c_v = \rho \cdot C \quad (3)$$

In these equations, λ represents the thermal conductivity, ρ is the density, C is the mass specific heat, κ the thermal diffusivity and c_v the volumetric specific heat capacity [20]. The declared thermo-physical properties of SiRPA at 500 K are reported in Table 2.

Bulk density	1.4±0.15 [g·cm^{-3}]
Volumetric specific heat capacity	1300±140 [kJ·m^{-3}·K^{-1}]
Thermal diffusivity	0.52 [mm^2·s^{-1}]
Thermal conductivity	0.67±0.07 [W·m^{-1}·K^{-1}]

Table 2. Thermo-physical properties of SiRPA at 500 K [21]

3 Simulation analysis on the potential of different Piston Thermal Barrier Coatings

In the first stage of the research activity, engine cycle simulation has been employed for assessing the potential of the thermal insulation technology, analyzing different piston coating materials.

A one-dimensional (1D) CFD commercially available software, developed by Gamma Technologies, GT-SUITE, was used for the simulations. The one-dimensional Navier-Stokes equations (conservation of continuity, momentum, and energy) are implemented in the simulation code [31]. A predictive multi-zone combustion model, DIPulse [32], created by Gamma Technology, was adopted for the burn rate prediction. A flow-based heat transfer model, developed by T. Morel and R. Keribar [33] was used for the convective Heat Transfer Coefficient (HTC) calculation. This model allows a more accurate estimation of the heat fluxes distribution between the engine components than the traditional heat transfer models (Woschni, Annand, etc.), as indicated in [33]. More in details, it is based on the in-cylinder flow field, including swirl motion and turbulence, which is not spatially uniform, so, it can address the complex Low Heat Rejection Engine issues. Further details and a comparison between Flow and Woschni models can be found in [34].

The 1D CFD engine model was directly coupled with an engine thermal model, representing the engine structure. In this way, the temperature calculation of the combustion chamber surfaces was possible. The thermal model approach is zero-dimensional: the engine components (pistons, liners, head, valves, etc.) are discretized in lumped thermal masses, characterized by their intensive properties (mass, density, areas, thermal conductivity, specific heat, and temperature). The model also takes into account the convection heat transfer between the structure, the coolant, and the oil.

The main feature of the developed thermal model is the wall temperature swings calculation through a transient heat conduction code. In particular, for low-

thermal-conductivity and low-heat-capacity materials, as the TBCs, the wall temperature swings are much higher respect to those produced by the traditional metal materials, therefore the transient effects cannot be neglected [4,35–37].

As mentioned above, the 1D CFD engine model and the 0D thermal model are directly coupled within the GT-SUITE platform. Precisely, the convective HTCs and the gas temperature, calculated with the engine model are directly used as boundaries in the thermal model, vice versa, the surface temperatures (transient within the engine cycle) are calculated with the thermal model and, then, are imposed in the engine model as boundaries. The process is iterative until the two models reach the convergence.

3.1 Case study

A turbocharged, direct injection, four-cylinder automotive diesel engine with high/low pressures cooled EGR systems has been used in this work. The engine version used in this research presents an electronic actuated Variable Geometry Turbine (VGT), a common rail fuel injection system capable of 2000 bar injection pressure, a chain-driven dual overhead camshaft. Engine block, cylinder head and pistons are all made of aluminum alloy. Specifications of the test engine are presented in Table 3.

Engine Type	Direct-Injection Diesel
Configuration	In-Line 4 Cylinders
Maximum Torque	320 Nm (at 2000 rpm)
Maximum Power	100 kW (at 4000 rpm)
Displacement	1598 cm^3
Compression Ratio	16:1
Bore x Stroke	79.7 mm x 80.1 mm
Injection system	Common Rail
Turbocharging system	Variable Geometry Turbine (VGT)

Table 3. Test engine specifications.

Four different engine operating points have been selected for the numerical analysis (engine speed [rpm] x BMEP [bar]): 1500x5, 2000x8, 2750x12, 2000x16. Once the model has been validated with the experimental data, it was used to study the effects of different Thermal Barrier Coatings applied on the entire piston surface. Further details on the model validation can be found in [34].

Two different TBC materials were chosen for the analysis: one representing the innovative Temperature Swing coatings (the anodized aluminum) and another representing the traditional ceramic coatings (the Yttria-Partially Stabilized Zirconia).

3.2 Simulation results

Literature values for the anodized aluminum and Y-PSZ properties are used in this numerical study, as reported in Table 4. As described in Section 2.2, the anodized aluminum is a particular coating obtained by the anodization of an aluminum alloy and characterized by a very porous structure, due to the presence of cylindrical nano-channels, oriented perpendicularly to the surface. Because of its porosity, the material presents very low density, thermal conductivity and heat capacity, which ensure high wall temperature swings. While, Y-PSZ is characterized by higher thermal conductivity and heat capacity respect to the anodized aluminum, which make the material less compliant with the temperature swing technique.

The thickness of 100 µm resulted in the optimum compromise between the insulation property during the combustion and the volumetric efficiency deterioration, as illustrated in [20,36,38]. In particular, thinner coatings present lower wall temperature peek, which lead to bad insulation effect, on the other hand, thicker coatings show charge air heating and worsening in pumping losses due to the higher wall temperature during the intake phase.

	Anodized aluminum	**Y-PSZ**
Density [$kg \cdot m^{-3}$]	1400	5650
Volumetric specific heat capacity [$kJ \cdot m^{-3} \cdot K^{-1}$]	1300	3500
Thermal conductivity [$W \cdot m^{-1} \cdot K^{-1}$]	0.67	1.4
TBC thickness [µm]	100	100

Table 4. Thermo-physical properties of anodized aluminum [21] and Y-PSZ [39] TBCs.

Figure 2 shows the piston wall temperature swings, resulting from the simulations at 2000 rpm and 8 bar of BMEP.

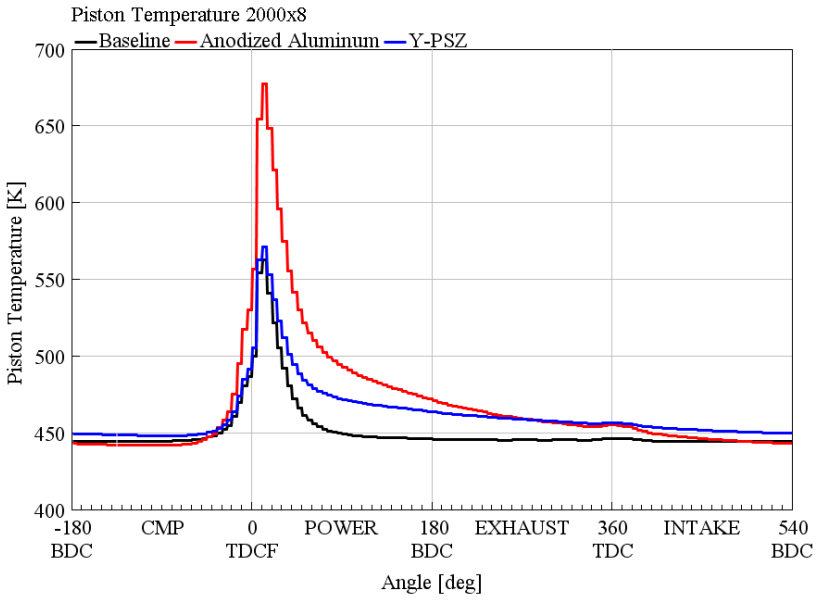

Figure 2. Piston wall temperature swings (anodized aluminum and Y-PSZ)

The anodized aluminum exhibits much greater wall temperature variations within the engine cycle respect to both the baseline and Y-PSZ. Consequently, it leads to heat loss reduction during combustion (thanks to the higher peak of wall temperature near the TDCF), keeping constant the intake mass and volumetric efficiency (thanks to the low wall temperature during the intake and compression strokes). Vice versa, Y-PSZ produces lower wall temperature during the combustion phase with respect to the anodized aluminum, because of its higher conductivity. Moreover, Y-PSZ presents a higher temperature during the intake due to its greater heat capacity in comparison with the anodized coating.

The potentialities in Heat Transfer and Indicated Specific Fuel Consumption reductions of both coatings are shown in Figure 3. The indicated quantities are used, rather than the brake ones, for excluding the effects of small friction variations.

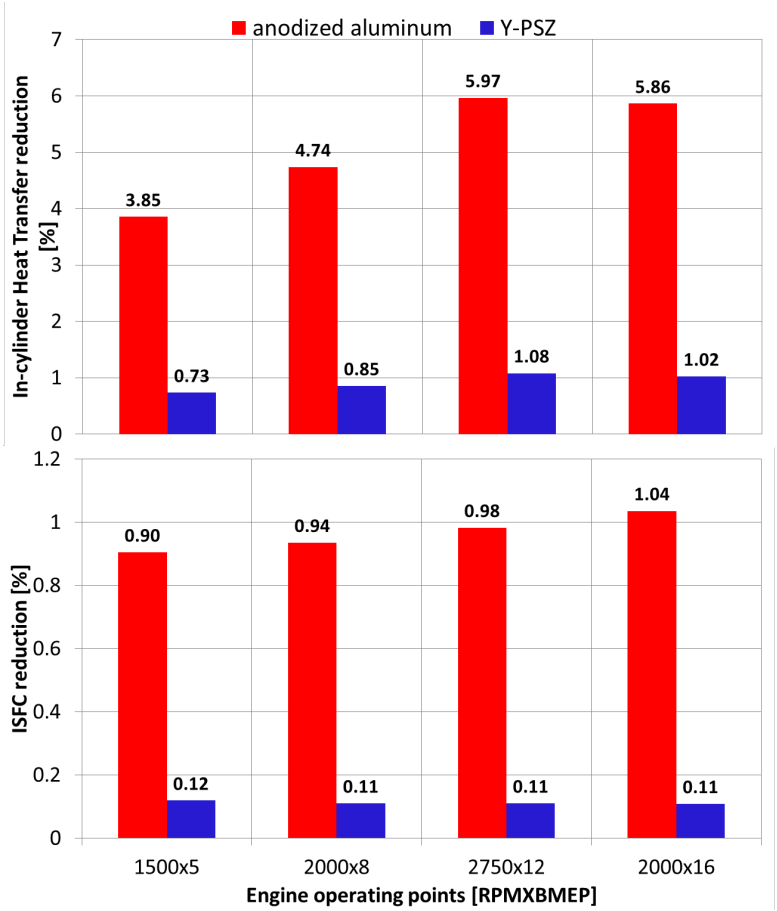

Figure 3. In-cylinder Heat Transfer reductions (top) and ISFC reductions (bottom) in case of 100µm anodized aluminum and Y-PSZ piston coatings.

The anodized aluminum TBC brings to more significant reductions in HT and ISFC due to its higher surface temperature swings. This behavior is confirmed for all the simulated operating points. However, the thermal insulation effect is more elevated at the higher loads and speeds, because of the higher gas temperature reached during the combustion in these points.

The simulations of two different materials as piston thermal barrier coatings have revealed that anodized aluminum has a bigger impact in heat transfer and ISFC

reductions (respectively until 6% and 1%), due to the greater temperature swing property of the material.

4 Experimental evaluation of the insulation performance

After the selection of the most promising piston coating through the numerical simulations, an experimental campaign was performed to assess the insulation potentialities in actual operating conditions.

4.1 Experimental apparatus

Experiments on the test engine (described in Section 3.1) were carried out at the Energy Department laboratory of Politecnico di Torino. Figure 4 shows a schematic diagram of the experimental setup.

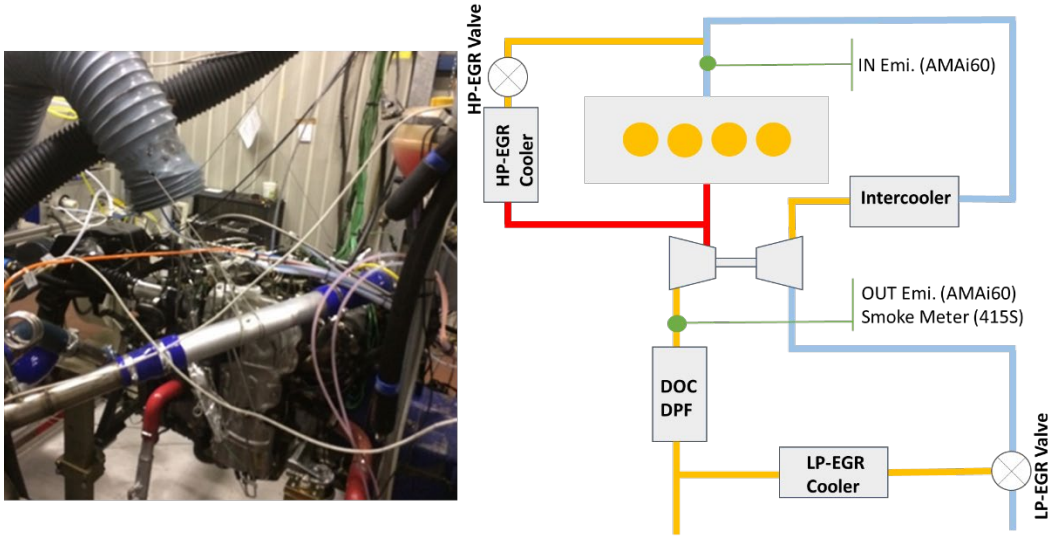

Figure 4. Engine test bench layout.

The engine was installed in a dynamic test bench equipped by a three-phase asynchronous dynamometer with controlled cabin and intake air temperature (25°C) and intake air humidity (50% RH).

The engine fuel consumption was measured by an AVL ® KMA 4000 continuous fuel mass flow meter; AVL ® AMA i60 was used for the measurement of the engine-out and intake gas compositions (NO, NOx, HC, CO, CO_2 and O_2) while an AVL ® 415S smoke meter was utilized for the measurement of Filter Smoke Number (FSN) of the engine-out gas. Pressure sensors and thermocouples are also used in several points of the engine like intake and exhaust pipelines, EGR lines, coolant, oil and fuel circuits. The engine cooling was ensured by a coolant to water heat exchanger in which the mains water was modulated by a PI controlled valve to target 90°C at the engine outlet. Similarly, the intercooler (see Figure 4) between the compressor and the intake manifold was an air to water regulated heat exchanger to target a pre-defined cooler outlet temperature.

Moreover, piezoelectric pressure transducers, mounted into the glow plug housings, are employed for the measurement of the in-cylinder pressures, which

are, then, acquired and post-processed through AVL ® IndiCom software. Finally, all the engine parameters were modified by a PC, connected to the ECU, using ETAS ® INCA software.

The precisions and linearities of the instrumentations are reported in Table 5.

Variable to measure	Sensors	Precision/Linearity
Fuel mass flow	AVL KMA 4000	0.1%
Torque	Dynamometer	0.3% FSO (525 Nm)
Gas analysis	AVL AMA i60	linearity 2%
FSN	AVL 415S	0.005 FSN + 3% meas. value
In-cylinder pressure	AVL GH13G	linearity 0.3% FSO

Table 5. Instrumentation precisions and linearities

Two different sets of pistons were evaluated: a conventional aluminum non-insulated configuration (Baseline) and a fully insulated configuration (named, Piston Full Coated – PFC), where the entire piston surface, including the cavity and the crown, was covered with an anodized aluminum coating. The characteristics of the tested TBC, reported in Table 6, are similar to those used for the simulations, compatibly with the manufacturer's specifications. Due to the high porosity of the coating, its surface roughness was considerably higher than the original aluminum (R_a 8 µm vs. R_a 3.2 µm). Figure 5 shows the front views of the two piston configurations.

Material	Anodized Aluminum
Thermal conductivity	0.9 [$W \cdot m^{-1} \cdot K^{-1}$]
Surface roughness (R_a)	8 [µm]
TBC thickness	90 [µm]

Table 6. Thermo-physical properties of PFC.

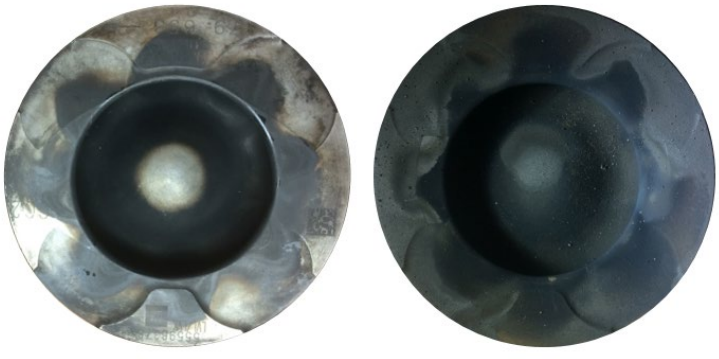

Baseline (Aluminum) *Piston Full Coated (PFC)*

Figure 5. Front views of the two piston configurations, after the experimental campaign.

4.2 Tests description

For assessing the potential of the thermal insulation technology, two different tests were performed, a Start of Injection (SOI) sweep and an Exhaust Gas Recirculation (EGR) sweep. Each test was repeated for four different engine operating points, covering middle-high speeds and loads of the engine: 1500x5, 2000x8, 2750x12, 2000x16 (engine speed [rpm] x BMEP [bar]). Moreover, each test was repeated on different days to improve the robustness of the results.

The SOI test consists of a sweep of five values of Start of Injection (SOI), depending on the operating point, while maintaining the other calibration parameters (i.e., intake pressure, rail pressure) fixed. Moreover, the pilot injection quantities and Exhaust Gas Recirculation (EGR) rate were set to zero to lower uncertainties in the measurements.

The EGR test was performed to assess the engine insulation impact on the combustion with high EGR rate. For all the operating points the SOI and the other calibration parameters were kept constant, and a sweep of EGR rate was performed. As far as the injection event is concerned, the pilot quantities were set to zero.

5 Results and discussion

5.1 Injection timing effects

The results of the SOI sweeps are shown in Figure 6. For sake of brevity, only the results of the lower and the higher tested engine loads (1500x5 and 2000x16, respectively) are reported. Average values over five tests performed in different days are analyzed.

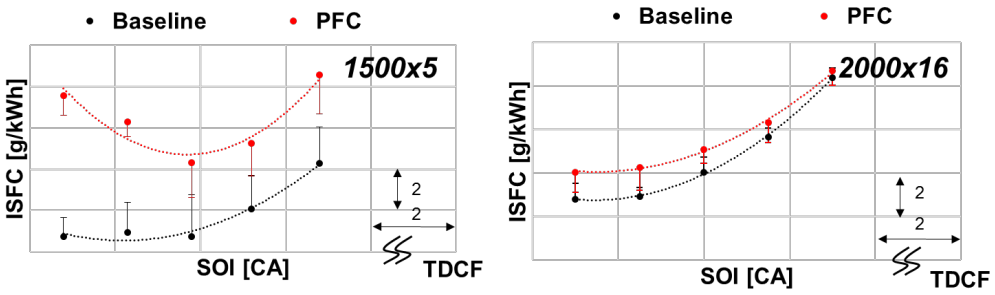

Figure 6. SOI sweep at 1500x5 (left), at 2000x16 (right). Average values over 5 tests performed in different days.

Unexpectedly, the worse Indicated Specific Fuel Consumption (ISFC) were obtained with the piston full coated configuration, especially at the lower load where ISFC increments higher than 2% were obtained. At the higher load, the gap between the two configurations is considerably smaller, below 1%. Moreover, the optimum injection timings move closer to the Top Dead Center Firing (TDCF) using the PFC configuration (better tolerance to the retarded injection).

In order to better understand the stated trend, a deeper analysis of the burn rates, calculated from the acquired in-cylinder pressures, was carried out.

As shown in Figure 7, the PFC configuration exhibits a slowdown in the late stage of combustion (during the mixing-controlled phase), probably due to the

interaction between the flame and the rough piston walls. In particular, as described in [20], in case of high roughness surfaces, the mixture motion near the walls slows down and its residence time in the piston bowl becomes longer. Consequently, high-temperature gasses stay longer time near the piston surface, causing an increment in the heat loss.

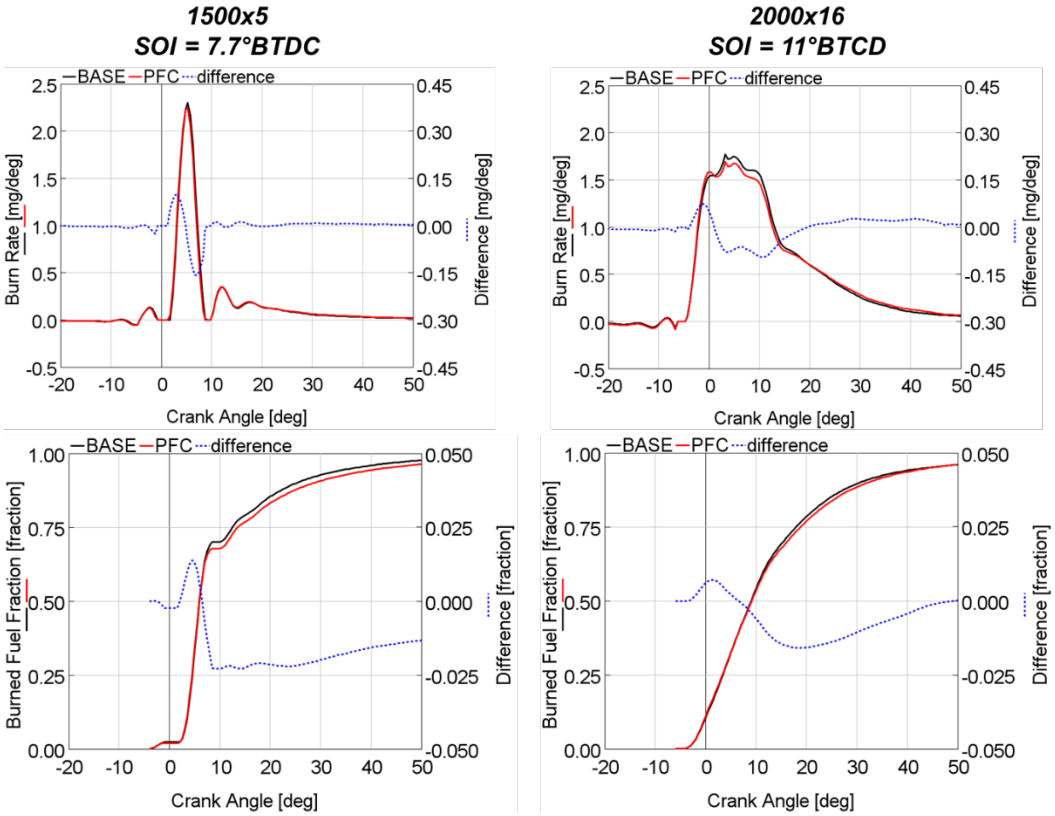

Figure 7. Burn Rate (top) and Burned Fuel Fraction diagram (bottom) at 1500x5 (left) and 2000x16 (right) without EGR. (Difference = PFC - BASE).

The first stage of the combustion (premixed phase) seems to be not affected by the TBC introduction, because in this phase there is still no interaction between the mixture and the wall. However, an unperceivable increase in the burned fuel fraction is found in this combustion stage with the PFC configuration, which can be ascribed to the higher in-cylinder temperature before the start of combustion, which can reduce the ignition delay of the mixture. For this reason, a faster-premixed combustion phase can compensate for the adverse effect of a retarded injection timing (better tolerance to the retarded injection).

The effects of the insulated piston on NO_x and soot emissions are shown in Figure 8. Piston coating technology does not seem to affect NO_x emissions, while soot emissions result increased. This trend could be explained by the different flame-wall interactions of the two configurations, which can affect the soot oxidation process.

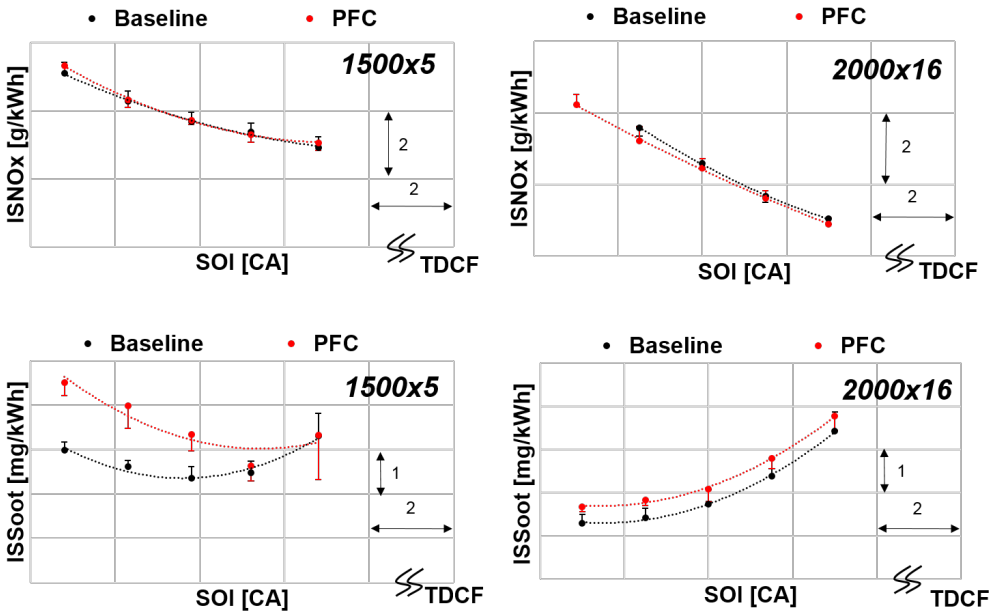

Figure 8. NOx (top) and SOOT (bottom) emissions as a function of the injection timing at 1500x5 (left) and at 2000x16 (right). Average values over 5 tests performed in different days.

5.2 EGR effects

The Indicated Specific NO_x emissions vs. Indicated Specific Fuel Consumption ($ISNO_x$/ISFC tradeoff curves), obtained with the EGR sweeps, are displayed in Figure 9.

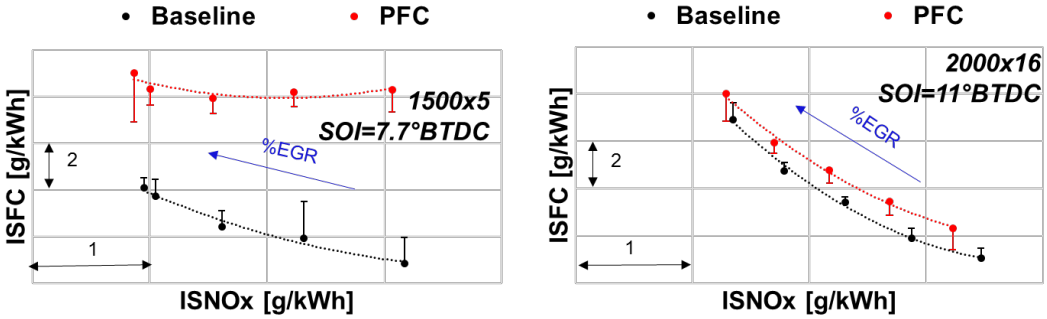

Figure 9. EGR sweep at 1500x5 (left) and at 2000x16 (right). Average values over 5 tests performed in different days.

Similarly to the SOI sweeps, the EGR sweeps show that the PFC configuration presents higher Indicated Specific Fuel Consumption (ISFC) than the baseline, reaching increment greater than 3% especially at lower load, speed and EGR rate. While, at higher load and EGR rate, the differences are significantly reduced (below 1%). Moreover, the PFC seems to be more tolerant to the EGR at the lower load, which can be explained through a more in-depth analysis of the burn rates, presented in Figure 10.

Also with the EGR, the mixing-controlled phase of the combustion goes slower with PFC configuration, caused by the interaction of the flame with the high-porous coating wall. As above said, this could bring to heat loss increase near the wall and indicated efficiency deterioration. On the other hand, the better EGR tolerance of PFC can be due to the faster initial stage of combustion around TDCF (premixed

phase), where the burned fuel fraction of PFC seems to be slightly greater than that of the baseline, which can be explained by the shorter ignition delay.

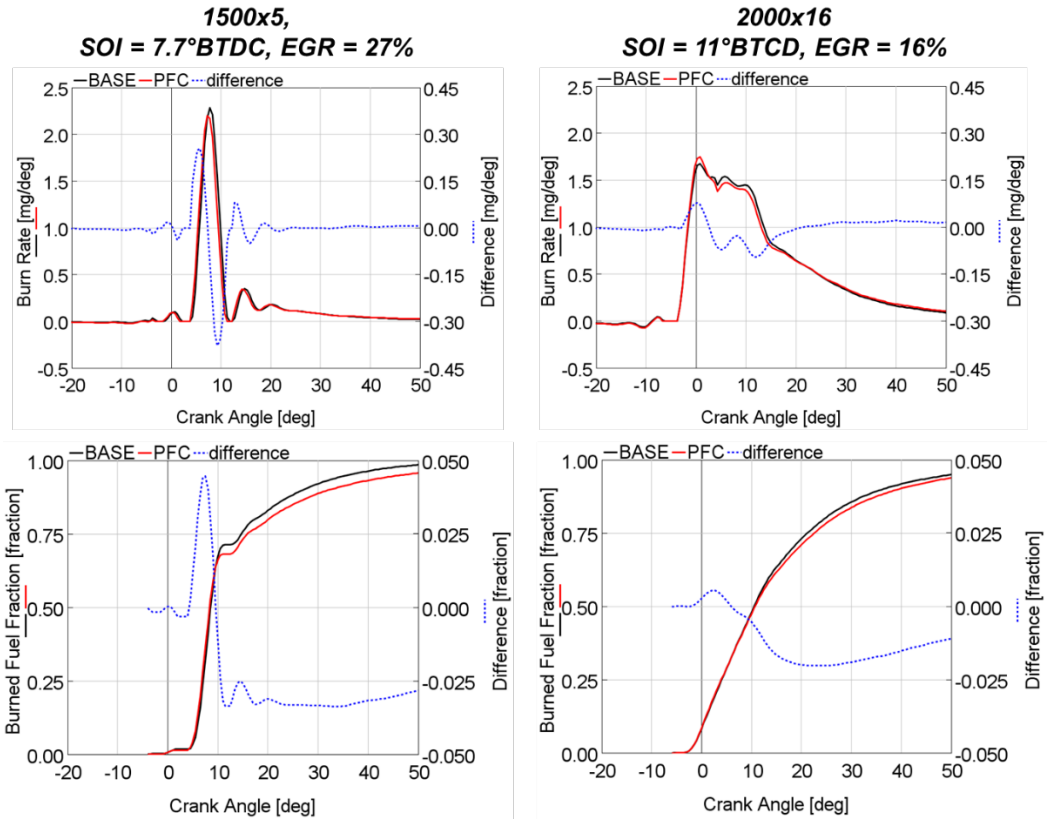

Figure 10. Burn Rate (top) and Burned Fuel Fraction diagram (bottom) at 1500x5 (left) and at 2000x16 (right) with EGR. (Difference = PFC – BASE).

The trade-off NO_x-SOOT, obtained through the EGR sweeps, are shown in Figure 11. At lower load, the tradeoff is more advantageous for the baseline configuration, because of its better combustion efficiency and more advantageous soot oxidation process. Vice versa, at higher load, where the indicated efficiencies and burn rates are comparable for both configurations, the tradeoff is slightly advantageous for the PFC, especially at higher EGR rates. This trend can be explained by the greater tolerance to the EGR, due to the reduction of the ignition delay.

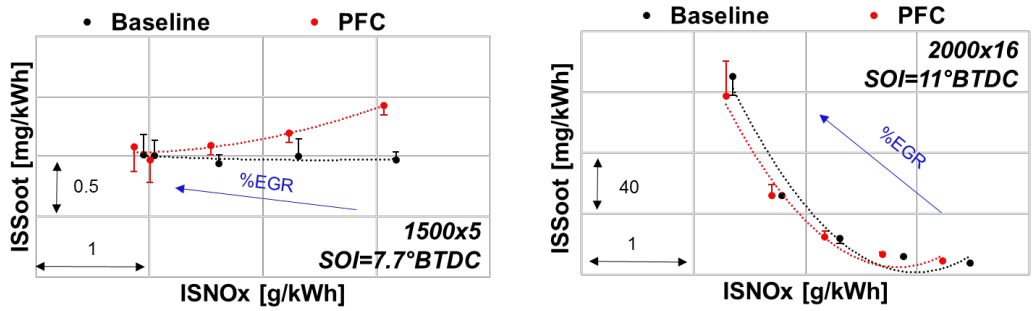

Figure 11. NO_x/SOOT tradeoff at 1500x5 (left) and at 2000x16 (right). Average values over 5 tests performed in different days.

6 Conclusions

Low Heat Rejection concept adopted on a passenger car diesel engine was assessed employing both the numerical simulation and the testing of a piston thermal barrier coating on a prototype engine. The main findings can be summarized as follows:

- Innovative TBCs (as anodized aluminum), characterized by low thermal conductivity and low heat capacity, have potentialities in improving fuel economy without any negative impact on pollutant emissions, due to their greater wall temperature swing, compared with the traditional ceramic TBCs (i.e. zirconia).
- The numerical simulation of the anodized aluminum as piston TBC have shown about 240 K of wall temperature swing, leading to approximately 4.7% in heat transfer reduction and 0.9% in indicated efficiency improvement, at middle load/speed engine operating condition (2000 rpm x 8 bar BMEP).
- The engine tests revealed that the worse indicated efficiency was obtained with the coated configuration, especially at the lower load where ISFC increments higher than 2% were obtained, while at the higher load, the gap between the two configurations was considerably reduced below 1%.
- The engine burn rates of coated configuration have shown shorter ignition delays, causing a shorter premixed combustion and a corresponding increase in the amount of fuel burned during the mixing controlled and late combustion phases. This slow-down of the combustion process was detrimental for combustion efficiency, overcoming the benefits obtained by a more adiabatic engine.
- The coated configuration resulted in a combustion process more tolerant to both retarded injection and EGR, thanks to the shorter ignition delay.
- Moreover, the porosity and the surface roughness of the coating (R_a 8 μm of coating vs. R_a 3.2 μm of aluminium) may have an effect in increasing the heat transfer and slowing down the combustion. However, these side effects cannot be captured with the 1D CFD engine model.
- Finally, slight differences in pollutant emissions occurred: with the PFC configuration, the soot resulted increased at the lower load, for the detrimental effect of the flame-wall interaction on the particulate oxidation process; while the NO_x emissions were slightly reduced, especially with EGR, for the diminished premixed combustion phase.

References

[1] T. Morel, E.F. Fort, P.N. Blumberg, Effect of Insulation Strategy and Design Parameters on Diesel Engine Heat Rejection and Performance, in: SAE Pap., 1985. doi:10.4271/850506.

[2] T. Morel, R. Keribar, P.N. Blumberg, E.F. Fort, Examination of Key Issues in Low Heat Rejection Engines, in: SAE Pap., 1986. doi:10.4271/860316.

[3] T. Morel, S. Wahiduzzaman, E.F. Fort, Heat transfer experiments in an insulated diesel engine, SAE Tech. Pap. (1988). doi:10.4271/880186.

[4] D.N. Assanis, J.B. Heywood, Development and Use of a Computer Simulation of the Turbocompounded Diesel System for Engine Performance and Component Heat Transfer Studies, SAE Pap. 860329 (1986). doi:10.4271/860329.

[5] Y. Miyairi, Computer Simulation of an LHR DI Diesel Engine, in: SAE Tech. Pap., SAE International, 1988. doi:10.4271/880187.

[6] D.D. Anderson, The Effects of Ceramic Port Insulation on Cylinder Head Performance in a Diesel Engine, in: SAE Tech. Pap., SAE International, 1996. doi:10.4271/961745.

[7] J.F. Tovell, The Reduction of Heat Losses to the Diesel Engine Cooling System, in: SAE Tech. Pap., SAE International, 1983. doi:10.4271/830316.

[8] C.D. Rakopoulos, G.C. Mavropoulos, COMPONENTS HEAT TRANSFER STUDIES IN A LOW HEAT REJECTION DI DIESEL ENGINE USING A HYBRID THERMOSTRUCTURAL FINITE ELEMENT MODEL, Appl. Therm. Eng. 18 (1998) 301–316. doi:1359-4311/98.

[9] C. Binder, F. Abou Nada, M. Richter, A. Cronhjort, D. Norling, Heat Loss Analysis of a Steel Piston and a YSZ Coated Piston in a Heavy-Duty Diesel Engine Using Phosphor Thermometry Measurements, SAE Int. J. Engines. (2017). doi:10.4271/2017-01-1046.

[10] E.M. Afify, D.E. Klett, The Effect of Selective Insulation on the Performance, Combustion, and NO Emissions of a DI Diesel Engine, in: SAE Tech. Pap., SAE International, 1996. doi:10.4271/960505.

[11] H. Aydin, Combined effects of thermal barrier coating and blending with diesel fuel on usability of vegetable oils in diesel engines, Appl. Therm. Eng. 51 (2013) 623–629. doi:10.1016/j.applthermaleng.2012.10.030.

[12] S. Aydin, C. Sayin, H. Aydin, Investigation of the usability of biodiesel obtained from residual frying oil in a diesel engine with thermal barrier coating, Appl. Therm. Eng. 80 (2015) 212–219. doi:10.1016/j.applthermaleng.2015.01.061.

[13] A. Parlak, A. Kolip, H. Yas, The effects of injection timing on NO x emissions of a low heat rejection indirect diesel injection engine, 25 (2005) 3042–3052. doi:10.1016/j.applthermaleng.2005.03.012.

[14] J.R. Serrano, F.J. Arnau, J. Martin, M. Hernandez, B. Lombard, Analysis of Engine Walls Thermal Insulation: Performance and Emissions, in: SAE Tech. Pap., SAE International, 2015. doi:10.4271/2015-01-1660.

[15] N. Uchida, H. Osada, A New Piston Insulation Concept for Heavy-Duty Diesel Engines to Reduce Heat Loss from the Wall, SAE Int. J. Engines. (2017). doi:10.4271/2017-24-0161.

[16] D.W. Dickey, The Effect of Insulated Combustion Chamber Surfaces on

Direct-Injected Diesel Engine Performance, Emissions and Combustion, in: SAE Int. Congr. Expo., SAE International, 1989. doi:https://doi.org/10.4271/890292.
[17] D.N. Assanis, K. Wiese, E. Schwarz, W. Bryzik, The Effects of Ceramic Coatings on Diesel Engine Performance and Exhaust Emissions, in: Int. Congr. Expo., SAE International, 1991. doi:https://doi.org/10.4271/910460.
[18] R. Kamo, W. Bryzik, Cummins–TARADCOM Adiabatic Turbocompound Engine Program, in: SAE Int. Congr. Expo., SAE International, 1981. doi:https://doi.org/10.4271/810070.
[19] T. Suziki, M. Tsujita, Y. Mori, T. Suzuki, An Observation of Combustion Phenomenon on Heat Insulated Turbo-Charged and Inter-Cooled D.I. Diesel Engines, in: 1986 SAE Int. Off-Highw. Powerpl. Congr. Expo., SAE International, 1986. doi:https://doi.org/10.4271/861187.
[20] A. Kawaguchi, H. Iguma, H. Yamashita, N. Takada, N. Nishikawa, C. Yamashita, Y. Wakisaka, K. Fukui, Thermo-Swing Wall Insulation Technology; - A Novel Heat Loss Reduction Approach on Engine Combustion Chamber -, in: SAE 2016 Int. Powertrains, Fuels Lubr. Meet., SAE International, 2016. doi:https://doi.org/10.4271/2016-01-2333.
[21] Y. Wakisaka, M. Inayoshi, K. Fukui, H. Kosaka, Y. Hotta, A. Kawaguchi, N. Takada, Reduction of Heat Loss and Improvement of Thermal Efficiency by Application of "Temperature Swing" Insulation to Direct-Injection Diesel Engines, SAE Int. J. Engines. 9 (2016) 1449–1459. doi:10.4271/2016-01-0661.
[22] H. Kosaka, Y. Wakisaka, Y. Nomura, Y. Hotta, M. Koike, K. Nakakita, A. Kawaguchi, Concept of "Temperature Swing Heat Insulation" in Combustion Chamber Walls, and Appropriate Thermo-Physical Properties for Heat Insulation Coat, SAE Int. J. Engines. 6 (2013) 142–149. doi:10.4271/2013-01-0274.
[23] T. Kogo, Y. Hamamura, K. Nakatani, T. Toda, A. Kawaguchi, A. Shoji, High Efficiency Diesel Engine with Low Heat Loss Combustion Concept - Toyota's Inline 4-Cylinder 2.8-Liter ESTEC 1GD-FTV Engine -, in: SAE Tech. Pap., SAE International, 2016. doi:10.4271/2016-01-0658.
[24] A. Broatch, P. Olmeda, X. Margot, J. Gomez-Soriano, Numerical simulations for evaluating the impact of advanced insulation coatings on H2 additivated gasoline lean combustion in a turbocharged spark-ignited engine, Appl. Therm. Eng. 148 (2019) 674–683. doi:10.1016/j.applthermaleng.2018.11.106.
[25] P. Andruskiewicz, P. Najt, R. Durrett, R. Payri, Assessing the capability of conventional in-cylinder insulation materials in achieving temperature swing engine performance benefits, Int. J. Engine Res. 19 (2018) 599–612. doi:10.1177/1468087417729254.
[26] X.Q. Cao, R. Vassen, D. Stoever, Ceramic materials for thermal barrier coatings, J. Eur. Ceram. Soc. (2004). doi:10.1016/S0955-2219(03)00129-8.
[27] R. Vaßen, M.O. Jarligo, T. Steinke, D.E. Mack, D. Stöver, Overview on advanced thermal barrier coatings, Surf. Coatings Technol. (2010). doi:10.1016/j.surfcoat.2010.08.151.
[28] K. Kokini, Y.R. Takeuchi, B.D. Choules, Surface thermal cracking of thermal barrier coatings owing to stress relaxation: Zirconia vs. Mullite, Surf. Coatings Technol. (1996). doi:10.1016/0257-8972(95)02647-9.
[29] A. Gilbert, K. Kokini, S. Sankarasubramanian, Thermal fracture of zirconia-mullite composite thermal barrier coatings under thermal shock: A numerical

study, Surf. Coatings Technol. (2008). doi:10.1016/j.surfcoat.2008.08.003.
[30] S. Rangaraj, K. Kokini, Interface thermal fracture in functionally graded zirconia-mullite-bond coat alloy thermal barrier coatings, Acta Mater. (2003). doi:10.1016/S1359-6454(02)00396-8.
[31] Gamma Technologies, GT-SUITE Help Manual, (2018).
[32] A. Piano, F. Millo, G. Boccardo, M. Rafigh, A. Gallone, M. Rimondi, Assessment of the Predictive Capabilities of a Combustion Model for a Modern Common Rail Automotive Diesel Engine, in: SAE Tech. Pap., SAE International, 2016. doi:10.4271/2016-01-0547.
[33] T. Morel, R. Keribar, A Model for Predicting Spatially and Time Resolved Convective Heat Transfer in Bowl-in-Piston Combustion Chambers, in: SAE Tech. Pap., SAE International, 1985. doi:10.4271/850204.
[34] S. Caputo, F. Millo, G. Cifali, F.C. Pesce, Numerical Investigation on the Effects of Different Thermal Insulation Strategies for a Passenger Car Diesel Engine, SAE Int. J. Engines. 10 (2017). doi:10.4271/2017-24-0021.
[35] C.D. Rakopoulos, D.C. Rakopoulos, G.C. Mavropoulos, E.G. Giakoumis, Experimental and theoretical study of the short term response temperature transients in the cylinder walls of a diesel engine at various operating conditions, Appl. Therm. Eng. 24 (2004) 679–702. doi:10.1016/j.applthermaleng.2003.11.002.
[36] A. Poubeau, A. Vauvy, F. Duffour, J.-M. Zaccardi, G. de Paola, M. Abramczuk, Modeling investigation of thermal insulation approaches for low heat rejection Diesel engines using a conjugate heat transfer model, Int. J. Engine Res. 20 (2019) 92–104. doi:10.1177/1468087418818264.
[37] P. Andruskiewicz, P. Najt, R. Durrett, S. Biesboer, T. Schaedler, R. Payri, Analysis of the effects of wall temperature swing on reciprocating internal combustion engine processes, Int. J. Engine Res. 19 (2018) 461–473. doi:10.1177/1468087417717903.
[38] D. Gatti, M. Jansons, One-Dimensional Modelling and Analysis of Thermal Barrier Coatings for Reduction of Cooling Loads in Military Vehicles, in: WCX World Congr. Exp., SAE International, 2018. doi:https://doi.org/10.4271/2018-01-1112.
[39] M. Durat, M. Kapsiz, E. Nart, F. Ficici, A. Parlak, The effects of coating materials in spark ignition engine design, Mater. Des. 36 (2012) 540–545. doi:10.1016/j.matdes.2011.11.053.